PERKIN 2

1,2-Migration in β-(acyloxy)ethyl radicals revisited—concerted or stepwise? †

Hendrik Zipse * and Michael Bootz

Department Chemie, Ludwig-Maximilians-Universität München, Butenandtstr. 13, D-83177 München, Germany. E-mail: zipse@cup.uni-muenchen.de

Received (in Cambridge, UK) 12th April 2001, Accepted 25th June 2001
First published as an Advance Article on the web 31st July 2001

The acyloxy rearrangement in 2-(acetyloxy)-2-methyl-1-propyl radical (**1a**) and in 2-(trifluoroacetyloxy)-2-methyl-1-propyl radical (**1b**) has been investigated with a number of theoretical methods. In both systems the most favorable reaction pathway for 1,2-acyloxy rearrangement leads through a five-membered ring transition state in a concerted fashion. A second pathway through a three-membered ring transition state is only slightly less favorable, while the addition–elimination process through a cyclic 1,3-dioxolan-2-yl radical intermediate has significantly higher barriers. Stationary points corresponding to a contact ion pair could not be found. With respect to the most favorable reaction pathway, the barrier difference between substrates **1a** and **1b** amounts to 2.5 ± 0.1 kcal mol^{-1} at a variety of theoretical levels. Solvent effects for the concerted pathways in hydrocarbon solvents, alcohols, and water have been calculated using the PCM scheme and found to be of rather limited magnitude. The barrier difference for reaction of **1a** in hydrocarbon solvents (cyclohexane, benzene) and in water was estimated to be around 1 kcal mol^{-1}. Based on kinetic isotope effects calculated for the [3,2]- and [1,2]-acyloxy rearrangement processes a differentiation of pathways is most easily possible through the strongly inverse deuterium isotope effects for d_2-labeling of the radical center in **1** and through the ratio of the ^{18}O isotope effects on the carboxylate oxygen atoms.

Introduction

The mechanism of rearrangement reactions in β-(acyloxy)ethyl radicals **1** has been controversial ever since its discovery.[1–3] The mechanistic options discussed up to date include (Scheme 1): **A**) reaction through a cyclization–ring opening sequence involving a five-membered ring intermediate **3**; **B**) concerted [3,2]-acyloxy rearrangement through a cyclic five-membered ring transition state **4**; **C**) concerted [1,2]-acyloxy rearrangement through a cyclic three-membered ring transition state **5**; and **D**) initial formation of a contact ion pair **6** followed by collapse to product radical **2**.

The experimentally used strategies to differentiate between these mechanistic options include: 1) isotopic labeling experiments with labeling of the carboxylate oxygen atoms being the preferred strategy;[4–6] 2) solvent effect studies in which only moderate rate effects have been found for a wide range of solvents, but a dramatic acceleration was noted in water;[7,8] 3) substituent effect studies that show substantial acceleration of the rearrangement rate through electron acceptors in the migrating carboxylate group and electron donors in the ethyl radical moiety of **1**;[1] 4) kinetic studies of putative dioxolanyl radical intermediates **3** showing that these species are most likely not located on the rearrangement pathway.[1] Early theoretical work by Radom *et al.*[9] as well as subsequent work by ourselves[10,11] has been in support of a concerted mechanism through a five-membered ring transition state. Analysis of the molecular orbitals along the reaction pathway suggested that the reaction can best be described as an intramolecular nucleophilic substitution reaction involving substantial charge separation.[10,11] With this classification in mind, one would expect that a stepwise S_N1-type process will become competitive in the presence of stabilizing substituents or more polar reaction media. Theoretical studies have, however, never been performed on systems that have also been studied experimentally. We are trying here to assess the situation for the 2-(acetyloxy)-2-methyl-1-propyl radical **1a** and the 2-(trifluoroacetyloxy)-2-methyl-1-propyl radical **1b**, two substrates that have been

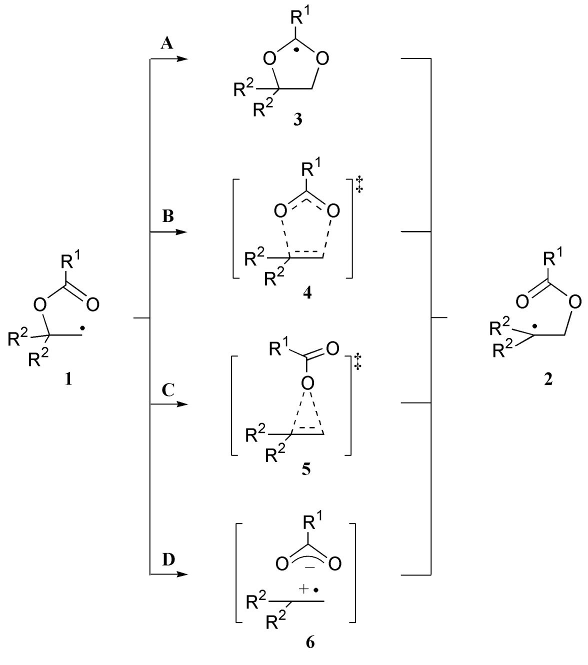

a $R^1 = CH_3$, $R^2 = CH_3$ **b** $R^1 = CF_3$, $R^2 = CH_3$
c $R^1 = CH_3$, $R^2 = H$ **d** $R^1 = CF_3$, $R^2 = H$

Scheme 1

---

† Electronic supplementary information (ESI) available: structural data, tables of absolute energies for stationary points in the rearrangement reactions of radicals **1a** and **1b** and absolute energies for fragments of **1a** and **1b**. See http://www.rsc.org/suppdata/p2/b1/b103324g/

DOI: 10.1039/b103324g

studied experimentally in some detail.[8] Rearrangement of **1a** was first studied by Tanner and Law who identified products derived from hydrogen transfer to both **1a** and its rearranged product **2a**.[2] Early EPR experiments by Beckwith *et al.* on **1a** in water led to the conclusion that the 1,2-migration process cannot possibly proceed through cyclic intermediates such as **3**.[12] A rough estimate for the rate of rearrangement of **1a** in water of $k_1(75\ °\mathrm{C}) = 3 \times 10^3\ \mathrm{s}^{-1}$ was also made at that time. Using the tin hydride method a value of $k_1(75\ °\mathrm{C}) = 6.2 \times 10^3\ \mathrm{s}^{-1}$ was later derived for reaction in benzene.[13] Kinetic EPR experiments later predicted a significantly smaller rate constant for rearrangement of **1a** in *tert*-butylbenzene of $k_1(75\ °\mathrm{C}) = 5.1 \times 10^2\ \mathrm{s}^{-1}$ along with Arrhenius parameters of $\log A(\mathbf{1a}) = 13.9 \pm 1.1\ \mathrm{s}^{-1}$ and $E_a(\mathbf{1a}) = +17.9 \pm 1.9$ kcal mol^{-1}. These results were taken to support a loose five-membered ring transition state involving substantial charge separation but no formation of intermediate ion pairs such as **6** or dioxolanyl radicals **3**.[8] These conclusions are also supported by a lower activation barrier of $E_a(\mathbf{1a}) = +12.7 \pm 1.2$ kcal mol^{-1} and smaller preexponential factor of $\log A(\mathbf{1a}) = 12.7 \pm 1.2\ \mathrm{s}^{-1}$ for reaction of **1a** in water, and by the significantly different Arrhenius parameters measured for **1b** in $CF_2ClCFCl_2$ solution of $\log A(\mathbf{1b}) = 11.0 \pm 1.0\ \mathrm{s}^{-1}$ and $E_a(\mathbf{1b}) = +9.8 \pm 1.2$ kcal mol^{-1}.

Computational methods

All quantum mechanical calculations have been performed with Gaussian 98.[14] Geometry optimizations have been performed with the hybrid Becke3LYP density functional as implemented in Gaussian 98 together with the standard split valence 6-31G(d) basis set.[15] Analytical second derivatives were used to calculate vibrational frequencies for all stationary points at this level. Combination of relative total energies calculated at this level with unscaled differences in zero point vibrational energies yields relative energies designated as "B3LYP/6-31G(d)". In all DFT calculations the pruned (99,590) grid provided as the "UltraFine" grid in Gaussian 98 has been used, since the default pruned (75,302) grid did not provide sufficient numerical accuracy for some parts of the calculations presented here. The charge distribution has been characterized through Mulliken as well as natural population analyses (NPA),[16] and by fitting the molecular electrostatic potential to atomic point charges using the CHELPG scheme.[17] The NPA values are discussed in the text, if not mentioned otherwise. Spin contamination is not a problem in all calculations based on the hybrid Becke3LYP functional as the $\langle S^2 \rangle$ expectation value never rose above 0.765 (transition state **5a**). Refined energies have been calculated using the G3(MP2)//B3LYP scheme of Curtiss *et al.* for some of the structures.[18] For the sake of comparison to the B3LYP/6-31G(d) results defined before, the G3(MP2)//B3LYP energies are also based on unscaled B3LYP zero point vibrational energies calculated with the enhanced grid size. Due to highly variable values of $\langle S^2 \rangle$ in the UHF calculations underlying the QCISD(T) and MP2 single points (up to 0.95 for transition state **5a**), the MP2 calculations needed for the basis set correction step in the G3 scheme were performed using a restricted reference (ROMP2). Solvent effects were included through single point calculations at Becke3LYP/6-31G(d) level of theory using the CPCM continuum solvation model.[19] The UAHF model has been used for the definition of the solute cavity.

Results

The lowest energy pathway found for rearrangement of radical **1a** leads through five-membered ring transition state **4a** (Scheme 2).

The reaction barrier of +11.3 kcal mol^{-1} (Table 1, B3LYP/6-31G(d) level) is substantially lower than the experimentally measured value of +17.9 kcal mol^{-1}. Similarly low or even lower values are obtained when larger basis sets are used, but a substantially higher value of +18.1 kcal mol^{-1} is predicted at the G3(MP2)//B3LYP level of theory (Table 1). Important structural characteristics of **4a** include two slightly different C–O bond distances of 2.09 Å (breaking bond) and 2.27 Å (forming bond), respectively (Fig. 1).

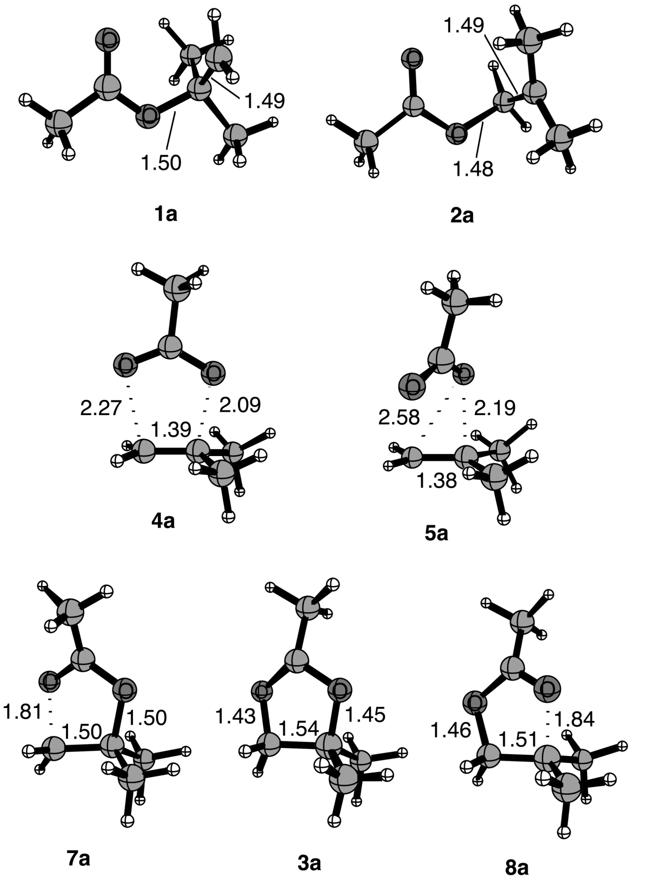

Fig. 1 Stationary points in the rearrangement of 2-(acetyloxy)-2-methyl-1-propyl radical **1a** (B3LYP/6-31G(d) level of theory).

All five centers intimately involved in the reactive process are located in one plane and the overall charge of the acetate group amounts to −0.36*e*. The closest alternative pathway for 1,2-acyloxy rearrangement in **1a** leads through three-membered ring transition state **5a** with a reaction barrier of +12.6 kcal mol^{-1}. Again the combined use of the B3LYP functional and larger basis sets leads to slightly lower activation barriers, while a barrier of +17.2 kcal mol^{-1} has been calculated at the G3(MP2)//B3LYP level of theory. The barrier difference between **4a** and **5a** is small at all levels of theory studied here, B3LYP calculations favoring **4a** and G3(MP2)//B3LYP favoring **5a**. Transition structure **5a** differs from **4a** in several aspects (Fig. 1). Most importantly, the acetoxy group is twisted out of the plane formed by the two ethylene carbon atoms and the migrating oxygen atom by 65°. The structure is also somewhat more dissociative in that the lengths of the breaking and forming C–O bonds of 2.19 Å and 2.58 Å, respectively, are significantly longer than the corresponding distances in **4a**. The charge distribution in **5a** is, however, quite comparable to **4a** with a carboxylate group charge of −0.35*e*. A third pathway leads along a stepwise ring closure–ring opening sequence through dioxolanyl radical **3a**. This intermediate is located approximately 11–13 kcal mol^{-1} above radical **1a** and can be reached through transition state **7a** with a barrier of 25–28 kcal mol^{-1}. Formation of the rearranged product **2a** proceeds through transition state **8a** located 12–16 kcal mol^{-1} above intermediate **3a**. These result are in clear support of all available experimental evidence ruling out the intermediacy of

Table 1 Relative energies ΔE_0 (in kcal mol^{-1}) for stationary points in the acyloxy shift of 2-(acetyloxy)-2-methyl-1-propyl radical (**1a**) and 2-(trifluoroacetyloxy)-2-methyl-1-propyl radical (**1b**)

R^1	Structure	B3LYP/ 6-31G(d)	B3LYP/ cc-pVDZ	B3LYP/ aug-cc-pVDZ	B3LYP/ cc-pVTZ	B3LYP/ aug-cc-pVTZ	G3(MP2)// B3LYP
CH_3	**1a**	0.0	0.0	0.0	0.0	0.0	0.0
	4a	+11.3	+10.6	+10.2	+9.9	+9.7	+18.1
	5a	+12.6	+12.0	+11.3	+10.8	+10.6	+17.2
	7a	+25.6	+25.4	+25.1	+26.4	+26.2	+28.1
	3a	+10.8	+11.4	+11.3	+12.7	+12.3	+11.7
	8a	+23.7	+23.6	+23.4	+24.6	+24.3	+27.3
	2a	−4.8	−4.7	−4.3	−4.8	−4.8	−0.5
	9 + **10**	+20.3	+19.3	+18.5	+16.4	+16.1	+27.5
	11 + **12**	+161.9	+162.4	+145.6	+151.2	+144.4	+160.9
CF_3	**1b**	0.0	0.0	0.0	0.0	0.0	0.0
	4b	+8.9	+8.2	+7.7	+7.5	+7.1	+15.7
	5b	+10.2	+9.5	+8.7	+8.2	+7.9	+18.6
	7b	+21.3	+21.3	+21.0	+22.2	+21.9	
	3b	+4.8	+5.4	+5.7	+7.1	+6.9	
	8b	+17.8	+17.7	+18.2	+19.3	+19.1	
	2b	−4.4	−4.3	−3.8	−4.4	−4.4	
	14 + **12**	+140.3	+140.5	+124.2	+130.1	+123.3	

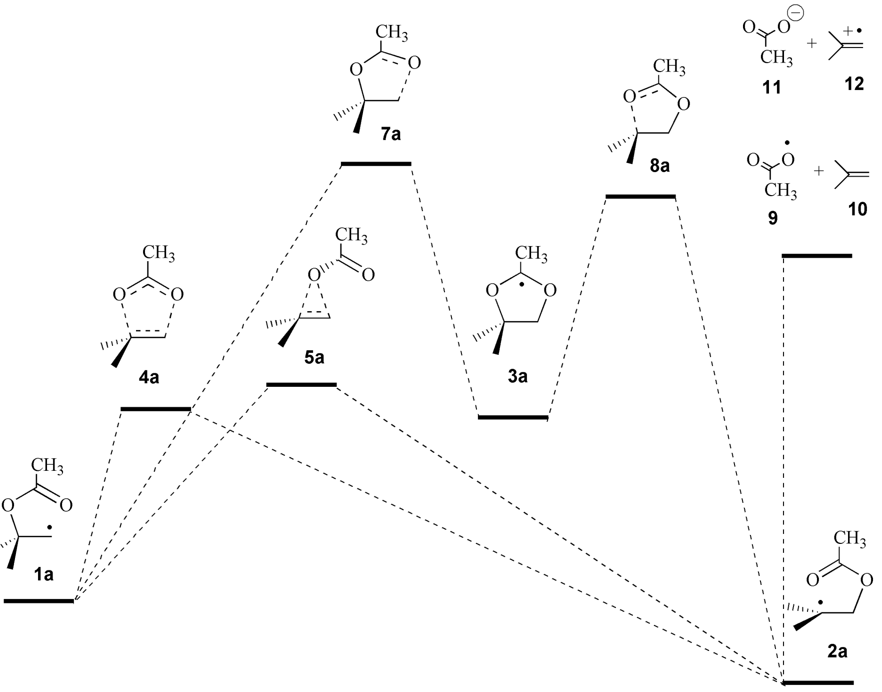

Scheme 2 Stationary points in the rearrangement of radical **1a** (B3LYP/6-31G(d) level of theory, drawn to scale).

dioxolanyl radical **3a** in the overall rearrangement process. The thermochemistry of the two conceivable C–O fragmentation processes have also been studied. Homolysis of the C–O bond in **1a** leading to acyloxy radical **9** and isobutene **10** is endothermic by at least 16 kcal mol^{-1}, while heterolysis to acetate **11** and isobutene radical cation **12** is, in the absence of any reaction medium, extremely unfavorable at +162 kcal mol^{-1}.

The potential energy surface calculated for rearrangement of the trifluoroacetate group in **1b** (Scheme 3) is rather similar to that found for **1a**. Reaction through five-membered ring transition state **4b** again provides the energetically most favorable reaction pathway. The barrier is slightly lower now at +8.9 kcal mol^{-1}, but the influence of changes in the computational methodology is the same as found for transition state **4a**. The five atoms involved in the bond breaking and bond making processes in **4b** are again all located in one plane, but the C–O distances are slightly longer now than in **4a** at 2.11 Å and 2.35 Å, respectively (Fig. 2). The carboxylate group charge amounts to −0.43*e*. Reaction through three-membered ring transition state **5b** is only slightly less favorable with a barrier of +10.2 kcal mol^{-1}. The energy difference between **4b** and **5b** is essentially independent of basis set choice and amounts to 0.7–1.3 kcal mol^{-1} at DFT level. The G3(MP2)//B3LYP barrier difference is much larger at 2.9 kcal mol^{-1} favoring transition state **4b**. The cyclization–ring opening pathway through dioxolanyl radical **3b** is again the least favorable of the three pathways, despite the fact that **3b** itself is located only 4.8 kcal mol^{-1} above **1b**. The much smaller energy difference between **1b** and **3b** as compared to the acetoxy analog has been observed before in smaller model systems and has been taken as a sign of captodative stabilization of trifluoromethyl substituted dioxolanyl radicals.[11] Transition state **7b** for formation of **3b** is, however, located 21 kcal mol^{-1} above **1b** and thus precludes efficient participation of this reaction channel. The subsequent transition state for ring opening **8b** is somewhat more favorable than **7b**, but still located 13 kcal mol^{-1} above intermediate **3b**. It is clear from these results that also for this system, the ring closure–ring opening sequence through cyclic dioxolanyl radicals will play no practical role in the 1,2-migration process. An estimate of the energetics of C–O bond homolysis in **1b** forming trifluoroacetyloxy radical **13** and isobutene **10** cannot be made as optimization of **13** leads to a weakly bound complex of carbon dioxide and trifluoromethyl radical at all levels studied here. Heterolytic cleavage of **1b** to trifluoroacetate **14** and isobutene radical cation **12** is again extremely unfavorable with a reaction energy of +140 kcal mol^{-1}. Stationary points corresponding to contact ion pair **6** could not be found for either of the two systems.

Discussion

A first point of comparison of experiment and theoretical prediction concerns the barrier difference in the 1,2-rearrangement reaction of **1a** and **1b**. The difference in the experimentally measured Arrhenius activation energies amounts to a respectable 6.9 ± 2.9 kcal mol^{-1}, but we have to note that the pre-exponential factors also vary quite significantly and that the Arrhenius correlations have been performed in somewhat different temperature ranges. Considering only the five-membered ring transition states **4a** and **4b**, the theoretically predicted barrier difference is very constant at 2.5 ± 0.1kcal mol^{-1}. Even if we take into account a possible involvement of the three-membered ring transition states **5a** and **5b**, the theoretically predicted barrier difference remains in only qualitative, but not quantitative agreement with the experimentally observed value.

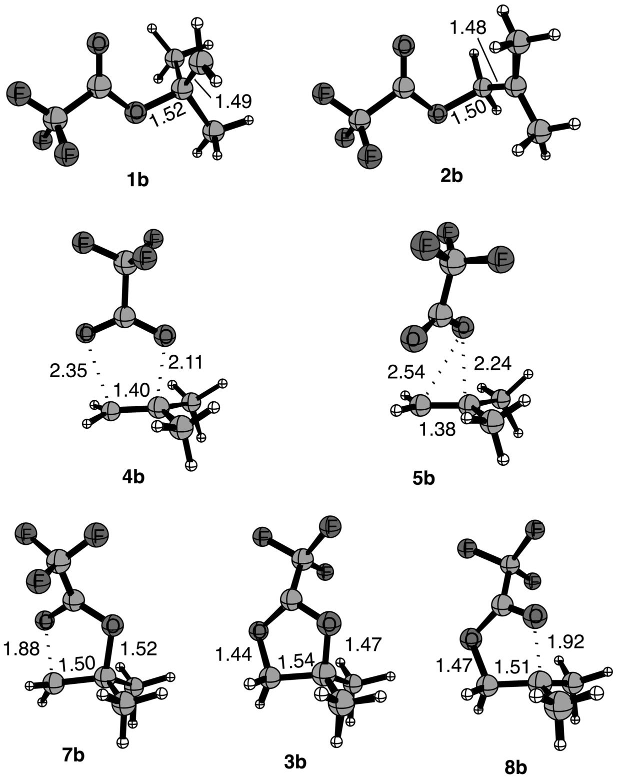

Fig. 2 Stationary points in the rearrangement of 2-(trifluoroacetyloxy)-2-methyl-1-propyl radical **1b** (B3LYP/6-31G(d) level of theory).

Table 2 Absolute and relative activation barriers for 1,2-acyloxy rearrangements through five- and three-membered ring transition states **4** and **5** as calculated at the B3LYP/6-31G(d) level of theory (in kcal mol^{-1})

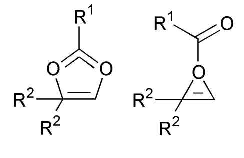

R^1	R^2	$\Delta E_0^‡(\mathbf{4})$	$\Delta E_0^‡(\mathbf{5})$	$\Delta\Delta E_0^‡$	Ref.
CH_3	H	+16.0	+18.4	+2.4	11
CF_3	H	+14.0	+17.3	+3.3	11
H	H	+13.7	+17.1	+3.4	11
CH_3	CH_3	+11.3	+12.6	+1.3	This work
CF_3	CH_3	+8.9	+10.2	+1.3	This work

The possible involvement of three-membered ring transition states **5a** and **5b** is, however, important in another respect. A survey of the B3LYP barrier differences between five- and three-membered ring transition states **4** and **5** as a function of the substitution pattern in Table 2 shows that reaction through the five-membered ring transition state **4** represents the most favorable pathway in all cases studied so far at the B3LYP level, but that transition state **5** becomes more competitive with lower absolute reaction barriers.

In addition, it appears that variation of acyl group substituent R^1 has a smaller effect on the **4**–**5** barrier difference than variations in alkyl substituents R^2. This is particularly relevant to acyloxy rearrangements in highly substituted systems, in which labeling experiments indicate a large degree

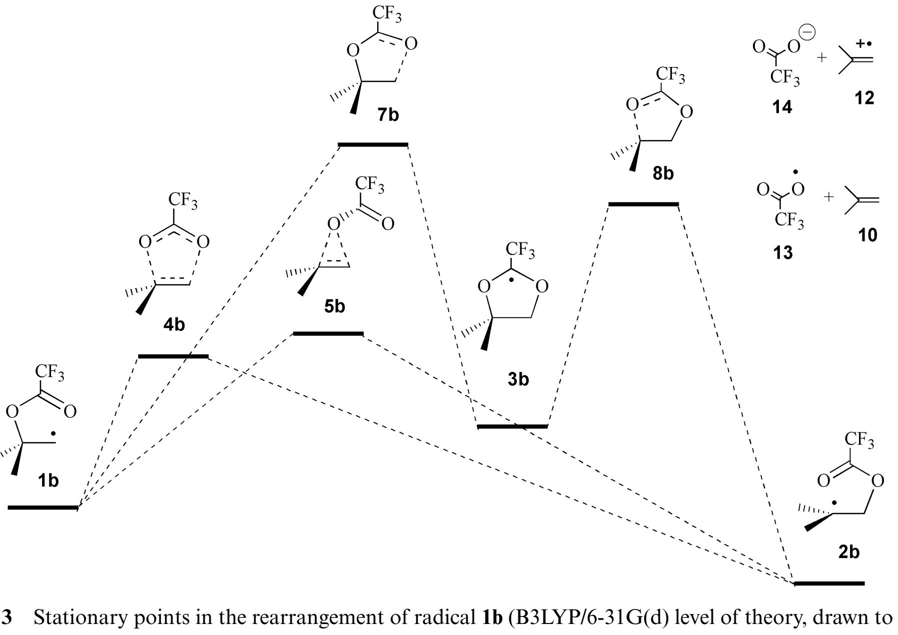

Scheme 3 Stationary points in the rearrangement of radical **1b** (B3LYP/6-31G(d) level of theory, drawn to scale).

Table 3 Carboxylate group charge in ground and transition states for rearrangement of various acyloxyethyl radicals

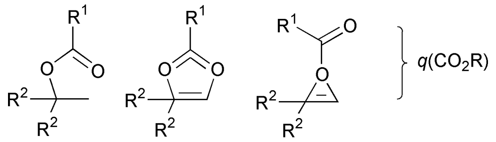

1 **4** **5**

R^1	R^2	**1**	**4**	**5**
Mulliken				
CH_3	H	−0.298	−0.285	−0.223
CF_3	H	−0.340	−0.343	−0.314
H	H	−0.308	−0.285	−0.246
CH_3	CH_3	−0.330	−0.346	−0.336
CF_3	CH_3	−0.379	−0.418	−0.413
CHELPG				
CH_3	H	−0.290	−0.261	−0.227
CF_3	H	−0.337	−0.332	−0.323
H	H	−0.313	−0.283	−0.261
CH_3	CH_3	−0.370	−0.357	−0.343
CF_3	CH_3	−0.434	−0.444	−0.423
NPA				
CH_3	H	−0.339	−0.297	−0.233
CF_3	H	−0.367	−0.349	−0.324
H	H	−0.341	−0.292	−0.253
CH_3	CH_3	−0.351	−0.357	−0.352
CF_3	CH_3	−0.386	−0.425	−0.426

of the [1,2]-shift process or reversible formation of contact ion pairs.[6,20]

Solvent and substituent effects in 1,2-acyloxy rearrangement reactions have been rationalized either by assuming substantial amounts of charge separation in transition states **4**[7,8] or by assuming initial formation of contact ion pairs.[1] The amount of charge separation can most conveniently be characterized through the overall partial charge of the acyloxy fragment in ground state **1** and transition states **4** and **5** as well as structural characteristics of these stationary points. As atomic charges depend to a large extend on the underlying computational methodology, our analysis is based on charges computed from a Mulliken population analysis, a natural population analysis (NPA), and on charges obtained by fitting the molecular electrostatic potential using the CHELPG scheme. In all cases the carboxylate group charge has been obtained as the sum over the partial charges of the contributing atomic centers (Table 3).

Despite the fact that partial atomic charges vary dramatically for single atomic centers, the overall carboxylate group charge is much less sensitive to changes in computational methodology. The partial charge of the central carbon atom in the trifluoromethyl group in **1b**, for example, varies from $+0.35e$ (CHELPG) over $+0.79e$ (Mulliken) to $+1.05e$ (NPA). The overall charge of the trifluoroacetyloxy group in the same structure is, in comparison, much less variable with values of $-0.43e$ (CHELPG), $-0.38e$ (Mulliken), and $-0.39e$ (NPA). Even though the following discussion is solely based on the NPA results, all trends are also visible in the Mulliken or CHELPG charge sets. The discussion will also include results obtained for smaller model systems from earlier studies.[10,11] Comparison of the charges calculated for ground state **1** with those for transition states **4** and **5** reveals that the acyloxy group charge is rather similar in ground and transition states for all systems described in Table 3. This also implies that factors leading to enhanced charge separation in transition states **4** and **5** (such as introduction of the trifluoromethyl group) have a similar influence already in ground state **1**. A more detailed analysis reveals that the carboxylate group charge decreases slightly on proceeding from ground state **1** to transition states **4** and **5** in the least reactive system ($R^1 = CH_3$, $R^2 = H$), while the transition states in the most reactive system ($R^1 = CF_3$, $R^2 = CH_3$) show a slightly larger carboxylate group charge than the corresponding ground state. In all cases the carboxylate group charge is larger in transition state **4** as compared to **5**, but the differences are fairly small and appear to vanish as the reaction barriers become lower. "Charge separation" in acyloxy migration processes should therefore primarily be understood as a consequence of structural differences between ground and transition states and not as a sudden increase in carboxylate group charge along the rearrangement pathway.

An indirect manifestation of the charge development along the reaction pathway is the solvent effect observed for **1a** with a barrier reduction of 5.2 ± 3.1 kcal mol^{-1} on moving from *tert*-butylbenzene to water as the reaction medium. Solvent effects on the rearrangement reactions of **1a** were studied through single point calculation of the solvation free energy ΔG_{solv} for ground state **1a** and transition states **4a** and **5a** in cyclohexane, benzene, and water using the CPCM scheme.[19] Transition state **4a** is slightly better solvated than transition state **5a** in all three solvents by 0.6 − 0.3 kcal mol^{-1}, supporting the importance of **4a** as the preferred reaction pathway even in solution. Lowering of the reaction barrier for the [3,2]-rearrangement process in cyclohexane and benzene is practically identical with $\Delta\Delta G_{solv}(\mathbf{1a}/\mathbf{4a}) = -0.5$ kcal mol^{-1}, while the effect is larger in water with $\Delta\Delta G_{solv}(\mathbf{1a}/\mathbf{4a}) = -1.4$ kcal mol^{-1}. Taken together, these data predict the barrier difference for reaction of **1a** in typical hydrocarbon solvents and water to be on the order of 1 kcal mol^{-1}, in close agreement to theoretical results obtained earlier for smaller model systems and using different solvation models, but in disagreement with the experimentally measured values. One possible explanation for this discrepancy rests on the known propensity of acyloxy rearrangements for acid catalysis, which might play a role in the experiments conducted in the aqueous phase.[21,22]

Kinetic isotope effects have been used in the past to describe transition state structures in more detail.[23] We have therefore calculated kinetic isotope effects (KIEs) for reaction through transition states **4** and **5** for a series of different isotopic substitutions (Scheme 4): ^{13}C–^{12}C KIEs for the two carbon atoms in

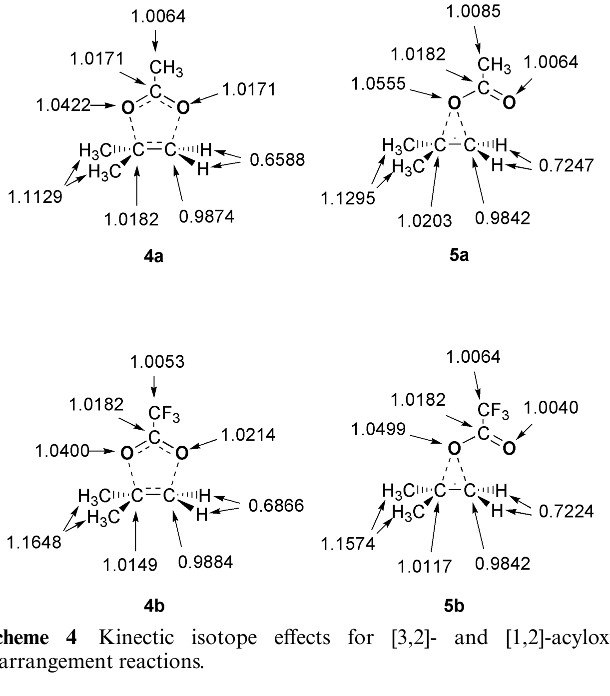

Scheme 4 Kinectic isotope effects for [3,2]- and [1,2]-acyloxy rearrangement reactions.

the acyloxy fragment as well as the two ethyl radical carbon atoms; ^{2}H–^{1}H KIEs for the two hydrogen atoms connected to the radical center in **1** (d$_2$) and the hydrogen atoms of the geminal methyl groups (d$_6$); ^{18}O–^{16}O KIEs for the two oxygen atoms in the acyloxy group.

As in earlier studies the calculation of isotope effects is based on the Eyring equation and differences in activation free energies obtained from harmonic vibrational frequency calculations at 298K.[23*a*,*b*,24] The largest effects for both rearrangement pathways result from deuterium labeling of both hydrogen atoms connected to the radical center in **1**. The most dramatic effect is found for transition state **4a** with a strongly inverse KIE(d$_2$) of 0.6588. This value results from the conformational restriction of the former radical center in the five-membered ring transition state **4a**. To a somewhat smaller extent this is also visible in three-membered ring transition state **5a** with a value of KIE(d$_2$) = 0.7247. Very similar values are found in the corresponding trifluoromethyl substituted transition states **4b** and **5b**. The conformational restriction of the former radical center in transition states **4** and **5** also appears to be responsible for the slightly inverse KIE of around 0.986 calculated for the corresponding carbon atom. Normal isotope effects of 1.012–1.020 are, in contrast, predicted for the newly forming radical center bearing the two methyl groups, the effects being slightly larger for the acetates than for the trifluoroacetates. Together with the d$_6$ KIEs for the two geminal methyl groups, which are also normal, these values reflect the increasing flexibility of the forming radical center. The KIEs calculated for the ^{18}O substitution in the carboxylate groups are reflective of the differing involvement of the oxygen atoms in transition states **4** and **5**. In transition states **4a** and **4b** both oxygen atoms participate in the bond making and breaking process and both centers show appreciable normal isotope effects, the values being larger for the breaking than the forming C–O bonds. In transition states **5a** and **5b**, however, a large and normal KIE is only predicted for the migrating oxygen atom, while only a very small KIE is present for the unreactive carbonyl oxygen atom. The ratio of the two ^{18}O-KIEs appears to be the most promising way to differentiate between the [3,2] and the [1,2] acyloxy rearrangements. Very small KIEs (below 1%) have also been obtained for the carbon atom of the carboxylate methyl groups. These centers might therefore be used as internal references for the experimental determination of KIEs.[23] Unfortunately, kinetic isotope effects cannot be calculated for the heterolytic pathway due to the lack of the corresponding transition state. However, if we assume the transition state for heterolysis to be late in terms of its nuclear and electronic structure, we can use the equilibrium isotope effects for ionic products **11** and **12** as an approximation for the KIEs of the heterolysis pathway. The most relevant values are those of 1.802 and 0.812 for deuteration of the methyl groups and the terminal methylene terminus, respectively, in radical cation **12**. Both can be used to differentiate heterolysis sufficiently well from the concerted pathways through **4** and **5**.

Conclusions

The energetically most favorable pathways for 1,2-acyloxy rearrangement in 2-(acyloxy)ethyl radicals **1a** and **1b** lead through five-membered ring transition states **4a** and **4b**. The corresponding three-membered ring transition states **5a** and **5b** are energetically slightly less favorable, but become more competitive with lower absolute reaction barriers. Reaction through intermediate formation of cyclic 1,3-dioxolanyl radicals **3** can safely be excluded for both systems studied here. The large barrier difference of 6.9 ± 2.9 measured experimentally for acyloxy migration in **1a** and **1b** contrasts with a theoretically predicted difference in reaction barriers of 2.5 ± 0.1 kcal mol^{-1} in the gas phase at several different theoretical levels. Solvent effects, even those for reaction in water, are predicted to be of minor relevance for both concerted pathways with small advantages for five-membered ring transition states **4**. This suggests that other factors might be responsible for the large rate acceleration observed experimentally for reaction of **1a** in water. Finally the theoretically predicted kinetic isotope effects show that transition states **4** and **5** are characterized through strongly inverse deuterium KIEs at the radical center C–H bonds and that **4** and **5** can be distinguished through the ratio of the ^{18}O KIEs for the acyloxy oxygen atoms.

Acknowledgements

We gratefully acknowledge continuing financial support of our research through the Fonds der Chemischen Industrie. Thanks are also due to Professor M. Newcomb (Wayne State University, Detroit) and Professor D. Crich (University of Illinois at Chicago) for fruitful discussion.

References

1 A. L. J. Beckwith, D. Crich, P. J. Duggan and Q. Yao, *Chem. Rev.*, 1997, **97**, 3273.
2 D. D. Tanner and F. C. P. Law, *J. Am. Chem. Soc.*, 1969, **91**, 7535.
3 J. M. Surzur and P. C. R. Teissier, *C. R. Acad. Sci., Ser. C*, 1967, **264**, 1981.
4 D. Crich and G. F. Filzen, *J. Org. Chem.*, 1995, **60**, 4834.
5 A. L. J. Beckwith and P. J. Duggan, *J. Chem. Soc., Perkin Trans. 2*, 1993, 1673.
6 A. L. J. Beckwith and P. J. Duggan, *J. Chem. Soc., Perkin Trans. 2*, 1992, 1777.
7 A. L. J. Beckwith and P. J. Duggan, *J. Am. Chem. Soc.*, 1996, **118**, 12838.
8 (*a*) L. R. C. Barclay, D. Griller and K. U. Ingold, *J. Am. Chem. Soc.*, 1982, **104**, 4399; (*b*) L. R. C. Barclay, J. Lusztyk and K. U. Ingold, *J. Am. Chem. Soc.*, 1984, **106**, 1793.
9 S. Saebo, A. L. J. Beckwith and L. Radom, *J. Am. Chem. Soc.*, 1984, **106**, 5119.
10 H. Zipse, *J. Chem. Soc., Perkin Trans. 2*, 1996, 1797.
11 H. Zipse, *J. Am. Chem. Soc.*, 1997, **119**, 1087.
12 A. L. J. Beckwith and P. K. Tindal, *Aust. J. Chem.*, 1971, **24**, 2099.
13 A. L. J. Beckwith and C. B. Thomas, *J. Chem. Soc., Perkin Trans. 2*, 1973, 861.
14 Gaussian 98, Revision A.6, M. J. Frisch, G. W. Trucks, H. B. Schlegel, G. E. Scuseria, M. A. Robb, J. R. Cheeseman, V. G. Zakrzewski, J. A. Montgomery, Jr., R. E. Stratmann, J. C. Burant, S. Dapprich, J. M. Millam, A. D. Daniels, K. N. Kudin, M. C. Strain, O. Farkas, J. Tomasi, V. Barone, M. Cossi, R. Cammi, B. Mennucci, C. Pomelli, C. Adamo, S. Clifford, J. Ochterski, G. A. Petersson, P. Y. Ayala, Q. Cui, K. Morokuma, D. K. Malick, A. D. Rabuck, K. Raghavachari, J. B. Foresman, J. Cioslowski, J. V. Ortiz, B. B. Stefanov, G. Liu, A. Liashenko, P. Piskorz, I. Komaromi, R. Gomperts, R. L. Martin, D. J. Fox, T. Keith, M. A. Al-Laham, C. Y. Peng, A. Nanayakkara, C. Gonzalez, M. Challacombe, P. M. W. Gill, B. Johnson, W. Chen, M. W. Wong, J. L. Andres, C. Gonzalez, M. Head-Gordon, E. S. Replogle, and J. A. Pople, Gaussian, Inc., Pittsburgh PA, 1998.
15 (*a*) A. D. J. Becke, *Chem. Phys.*, 1993, **98**, 5648; (*b*) C. Lee, W. Yang and R. G. Parr, *Phys. Rev. B*, 1988, **37**, 785.
16 A. E. Reed, L. A. Curtiss and F. Weinhold, *Chem. Rev.*, 1988, **88**, 899.
17 C. M. Breneman and K. B. Wiberg, *J. Comput. Chem.*, 1990, **11**, 361.
18 A. G. Baboul, L. A. Curtiss, P. C. Redfern and K. Raghavachari, *J. Chem. Phys.*, 1999, **110**, 7650.
19 (*a*) N. Rega, M. Cossi and V. Barone, *J. Chem. Phys.*, 1996, **105**, 11060; (*b*) V. Barone, M. Cossi and J. Tomasi, *J. Chem. Phys.*, 1997, **107**, 3210; (*c*) M. Cossi and V. Barone, *J. Phys. Chem. A*, 1998, **102**, 1995.
20 P. Kocovsky, I. Stary and F. Turecek, *Tetrahedron Lett.*, 1986, **27**, 1513.
21 H. Zipse, *Acc. Chem. Res*, 1999, **32**, 571.
22 E. Lancote and P. Renaud, *Angew. Chem.*, 1998, **110**, 2369 (*Angew. Chem., Int. Ed.*, 1998, **37**, 2259).
23 (*a*) I. H. Williams, *J. Am. Chem. Soc.*, 1984, **106**, 7206; (*b*) S. S. Glad and F. Jensen, *J. Am. Chem. Soc.*, 1994, **116**, 9302; (*c*) O. Wiest, K. A. Black and K. N. Houk, *J. Am. Chem. Soc.*, 1994, **116**, 10336;

(*d*) L. P. Olson, Y. Li, K. N. Houk, A. J. Kresge and L. J. Schaad, *J. Am. Chem. Soc.*, 1995, **117**, 2992; (*e*) O. Wiest, K. N. Houk, K. A. Black and B. Thomas IV, *J. Am. Chem. Soc.*, 1995, **117**, 8594; (*f*) H. Zipse, G. Apaydin and K. N. Houk, *J. Am. Chem. Soc.*, 1995, **117**, 8608; (*g*) E. Goldstein, B. R. Beno and K. N. Houk, *J. Am. Chem. Soc.*, 1996, **118**, 6036; (*h*) B. R. Beno, K. N. Houk and D. A. Singleton, *J. Am. Chem. Soc.*, 1996, **118**, 9984; (*i*) D. A. Singleton, S. R. Merrigan, J. Liu and K. N. Houk, *J. Am. Chem. Soc.*, 1997, **119**, 3385; (*j*) A. J. DelMonte, J. Haller, K. N. Houk, K. B. Sharpless, D. A. Singleton, T. Strassner and A. A. Thomas, *J. Am. Chem. Soc.*, 1997, **119**, 9907; (*k*) K. N. Houk and T. Strassner, *J. Org. Chem.*, 1999, **64**, 800.

24 M. Newcomb, J. H. Horner, P. O. Whitted, D. Crich, X. Huang, Q. Yao and H. Zipse, *J. Am. Chem. Soc.*, 1999, **121**, 10685.